Additive Manufacturing 10 (2016) 67–75

Contents lists available at ScienceDirect

Additive Manufacturing

journal homepage: www.elsevier.com/locate/addma

Full-length article

Influence of energy density on flexural properties of laser-sintered UHMWPE

Yas Khalil[a,*], Adam Kowalski[b], Neil Hopkinson[a]

[a] Department of Mechanical Engineering, The University of Sheffield, Sheffield S1 3JD, UK
[b] Unilever, R&D Port Sunlight Laboratory, Wirral CH63 3JW, UK

ARTICLE INFO

Article history:
Received 25 November 2015
Received in revised form 4 February 2016
Accepted 11 March 2016
Available online 14 March 2016

Keywords:
Additive manufacturing
UHMWPE
Laser sintering
Laser power
Flexural properties

ABSTRACT

Ultra High Molecular Weight Polyethylene (UHMWPE) is a semi-crystalline polymer that has remarkable properties of high mechanical properties, excellent wear resistance, low friction and chemical resistance, and it is found in many applications such sporting goods, medical artificial joints, bullet proof jackets and armours, ropes and fishing lines [1]. UHMWPE parts cannot be produced easily by many conventional processes because of its very high melt viscosity resulting from its very long chains [2]. Additive Manufacturing (AM) is moving from being an industrial rapid prototyping process to becoming a mainstream manufacturing process in a wide range of applications. Laser sintering of polymers is one of the AM techniques that is most promising process owing to its ability to produce parts with complex geometries, accurate dimensions, and good mechanical strength [3]. This paper reports attempts to laser-sinter UHMWPE and assesses the effects of laser energy density on the flexural properties of the sintered parts. The properties of the UHMWPE sintered parts were evaluated by performing flexural three point bending tests and were compared in terms of flexural strength, flexural modulus and ductility (deflection). Part dimensions and relative density were evaluated in order to optimise the laser sintering parameters. Thermal analysis of samples was made by differential scanning calorimetry (DSC) for the virgin powder. Results show that flexural strength, modulus and ductility are influenced by laser energy density and flexural strength and modulus of 1.37 MPa and 32.12 MPa respectively are still achievable at a lower laser energy density of 0.016 J/mm^2 (Laser power of 6 W). Part dimensions and bulk density are also influenced by laser energy density.

1. Introduction

1.1. Polymer laser sintering

Additive Manufacturing (AM), or 3D printing as it is more commonly referred to, is defined by the ISO Technical Committee 261 on Additive Manufacturing, in cooperation with ASTM Committee F42 on Additive Manufacturing Technologies, as "a process of joining materials to make parts from 3D model data, usually layer upon layer, as opposed to subtractive manufacturing and formative manufacturing methodologies" [4]. There are over twenty different recognised AM technologies based on the additive principle, but the method of layers consolidation may differs from one to another. Seven AM process categories were adapted by the ISO/TC 261 and ASTM/F42 [4]:

- Vat Photopolymerisation
- Material Jetting
- Binder Jetting
- Material Extrusion
- Powder Bed Fusion
- Sheet Lamination
- Directed Energy Deposition

AM is moving from being an industrial rapid prototyping technique to becoming a mainstream manufacturing process and a more demanding technology used by industry and consumers.

In Laser Sintering (LS), which is a powder bed fusion process, parts are built layer by layer using laser to sinter powdered material directly from three-dimensional (3D) computer aided design (CAD) models (Fig. 1). LS has the ability to produce parts with complex geometries, accurate dimensions, and good mechanical strength [3]. Controlled complex geometries can be achieved both externally and internally. These internal structures are highly

* Corresponding author.
E-mail address: y.khalil@sheffield.ac.uk (Y. Khalil).

http://dx.doi.org/10.1016/j.addma.2016.03.002

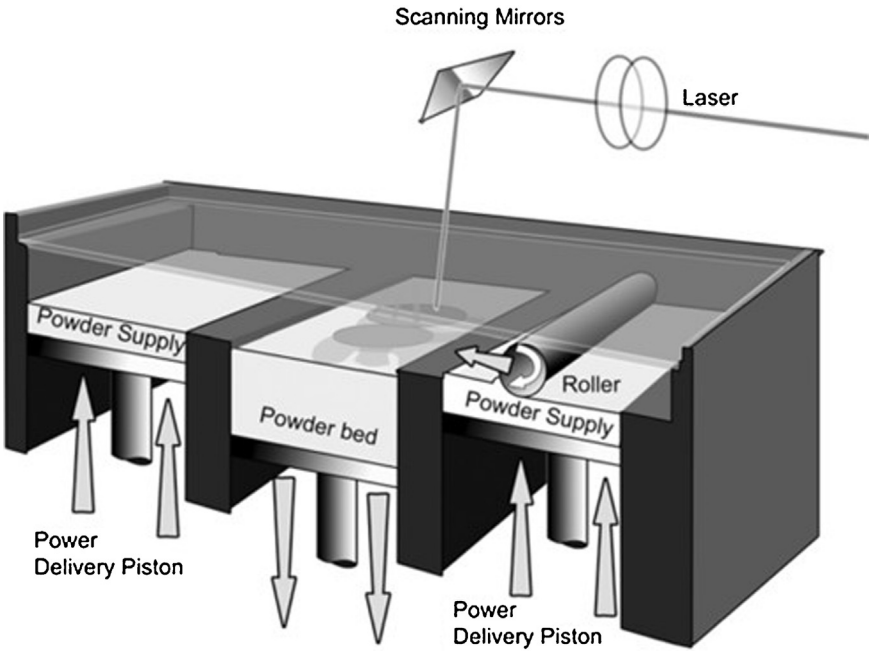

Fig. 1. Schematic of laser sintering machine [6].

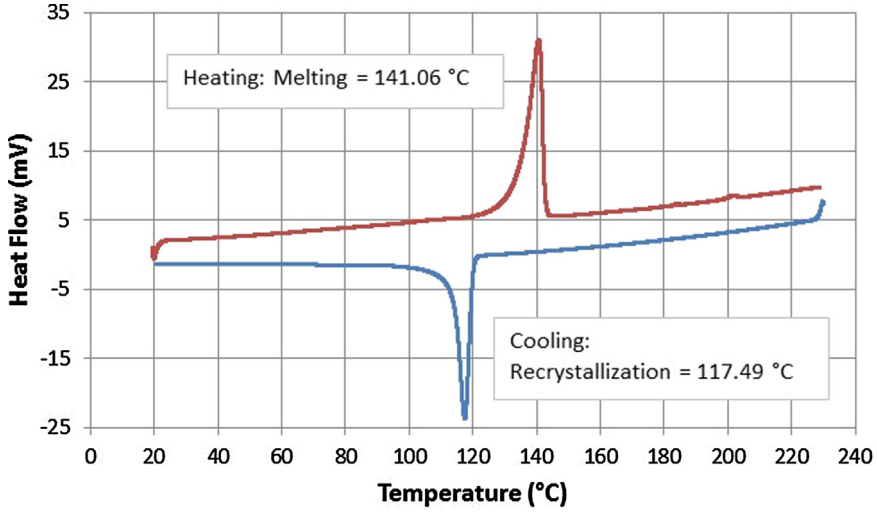

Fig. 2. DSC curve of UHMWPE powder (GUR 2122).

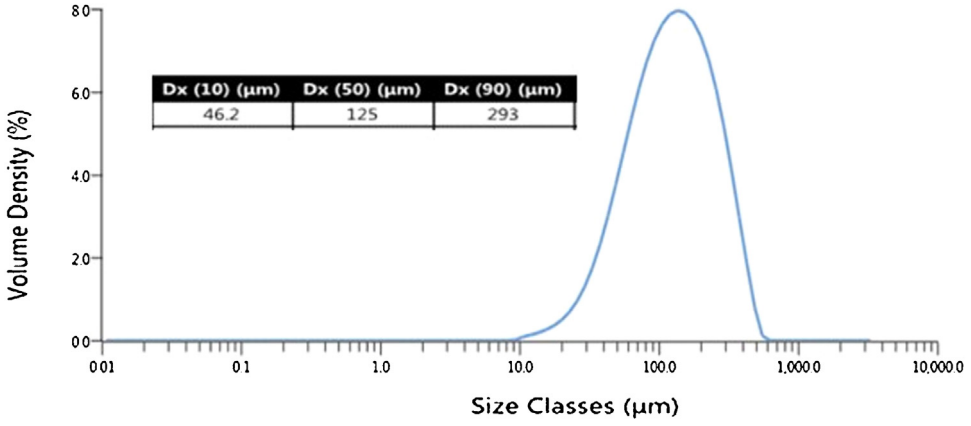

Fig. 3. Particle size distribution of UHMWPE (GUR 2122) powder.

regular and reproducible interconnected porous network that could provide excellent applications such as bone implant [5].

The principle of polymer LS can be summarised as follows:

- A LS machine lays down a thin layer of polymer powder in part-build area
- The powder is heated up with laser to fuse the powder with the previous layers
- After the laser has finished tracing one cross section of the model, a new load of powder is applied on top by roller or blade mechanism
- The process is repeated until the whole geometry is completed

LS build parameters include laser power, laser speed, scan spacing, powder layer thickness, number of scans, part bed temperature, feed bed temperature, build size, roller speed, time between layers, and heating-cooling rates [3].

1.2. Ultra high molecular weight polyethylene (UHMWPE)

UHMWPE is an engineering thermoplastic polymer that has remarkable properties of excellent abrasion resistance, self-lubrication property, fatigue resistance, impact resistance, high chemical stability, resistance to low temperature, and biocompatibility [7,8]. A conventionally processed UHMWPE has a density of 0.939 g/cm^3 and flexural strength and modulus of 14.4 MPa and 713 MPa respectively [9]. It is widely used in military, industrial, medical and consumer applications. UHMWPE is found in many applications to fabricate various products including pipes, panels, bars, shuttles, gears, artificial bones, body armour. However, UHMWPE is difficult to process by conventional melt processes such as injection moulding because of its high molecular weight which results in a very high melt viscosity [1,2,10].

A few attempts have been made to process UHMWPE using laser sintering technique. Rimell and Marquis [11] attempted to fabricate linear continuous UHMWPE (GUR 4120 and GUR 4170) solid layers for clinical application by using a non-commercial LS machine. However, they were unable to produce LS parts due to high degree of shrinkage and curling developed during the laser sintering process. However, Goodridge et al. [5] have successfully produced multilayer parts from UHMWPE (GUR 4170) using the commercial Vanguard Laser Sintering machine from 3D Systems. Goodridge et al. carried out a number of attempts to obtain suitable parameters for laser sintering of UHMWPE by using a range of laser power, bed and feed temperature and scan count. A precise laser power and bed and feed temperatures were required to fabricate UHMWPE parts due to its very narrow processing window. Goodridge et al. reported that the UHMWPE multilayer parts were produced only at a laser power of 13 W with a bed temperature of 135 °C, feed temperature of 125 °C, and double laser scan count. They investigated the mechanical properties of the sintered parts using three point bend tests (with support span length of 20 mm) and tensile test. The result shows that the LS parts have an average flexural strength of 0.52 ± 0.2 MPa with a modulus of 18.67 ± 4.3 MPa and Ultimate Tensile Strength (UTS) and Young's modulus were just above 0.2 MPa and 1.5 GPa respectively.

In this work, UHMWPE LS parts were successfully manufactured using various laser power. Sintered parts were manufactured with significant sintering between particles and layers and also good mechanical properties. Powder characterisation of raw powder has been carried out. Flexural and physical properties of the laser-sintered parts were compared and the resultant differences were discussed.

2. Material characterization methods

The UHMWPE powder used in manufacturing laser-sintered parts was GUR 2122 from Ticona, Celanese (Germany) with a reported average particle size of 130 ± 20 μm. GUR 2122 UHMWPE is a linear polyolefin with a molecular weight of around 4.5×10^6 g/mol. It has a unique morphology that produces a low bulk density of 0.20–0.25 g/cm^3 (Celanese GUR® 2122 UHMWPE datasheet).

2.1. Thermal analysis

A Perkin Elmer DSC 8500 was used to characterise the UHMWPE powder for the melting and crystallization behaviour at heating and cooling rates of 10 °C/min in nitrogen atmosphere. The start and end temperatures were 25 °C and 220 °C respectively and the weight of the sample was 6.3 mg in a sealed aluminium pan.

2.2. Particle size

Particle size was determined using Mastersizer 3000 (Malvern Instruments, UK), which uses laser diffraction to measure the size of particles. In this method the intensity of light scattered is measured as a laser beam passes through a dispersed particulate sample. The sample was characterised by dry powder dispersion method using air as a media. The distribution of the particle size was determined at a feed pressure of 3 bar and the run was selected to perform 10 measurements from the available sample. The size distributions were reported by the cumulative volume diameter at 10%, 50% and 90%.

2.3. Scanning electron microscopy (SEM)

Microstructure of the UHMWPE powder was examined using a scanning electron microscope (Philips XL-20, Holland) at an accelerating voltage of 10 kV. In order to prepare a sample for examination, a sample holder with an adhesive tape mounted on, was dipped in the powder and then was shaken up to remove the excess leaving a small number of particles. Sample was gold sputtered before the examination.

3. Material characterization results

3.1. Thermal analysis

The DSC curve for un-sintered UHMWPE powder is shown in Fig. 2. The melting temperature of the UHMWPE is around 141 °C and the peak for solidification is around 117 °C. This temperature was used to assist with the determination of the build temperature of the powder bed (i.e. processing window). UHMWPE processing window appears to be extremely narrow and could show a significant issue for commercial processing. Approximate temperatures of part bed and removal chamber were determined by monitoring the flow of the powder over the build area while the blade spreads the powder across the powder bed.

3.2. Particle size

Fig. 3 summarizes the UHMWPE particle size below 10%, 50%, and 90% of the particle diameters taken from the particle size distribution result. The average particle size of UHMWPE used in this work was 125 μm. 10% of the UHMWPE particles were larger than 293 μm, while almost 10% of the particles were less than 46.2 μm.

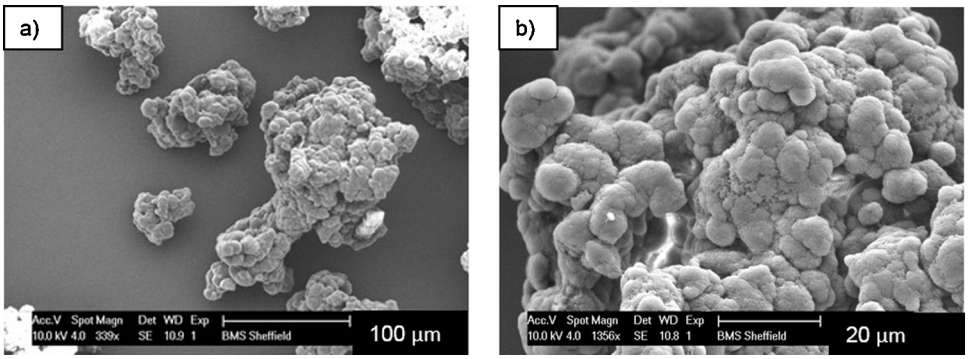

Fig. 4. SEM micrographs of un-sintered UHMWPE powder magnifications: (a) 339× and (b) 1356×.

Table 1
Laser sintering parameters.

Scan speed (mm/s)	Scan spacing (mm)	Powder bed temperature (°C)	Removal chamber temperature (°C)	Layer thickness (mm)	Laser count
2500	0.15	142	135	0.1	2

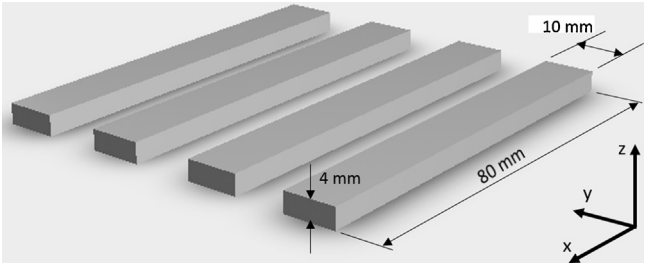

Fig. 5. Schematic of the orientation of the parts in the build bed.

3.3. Scanning electron microscopy (SEM)

SEM examination of UHMWPE powder shows that the particles are non-spherical in shape with highly agglomerated structure of smaller particles showing a cauliflower appearance (Fig. 4).

4. Parts manufacturing and characterization methods

4.1. Laser sintering

Before the sintering of the test samples of UHMWPE parts, a range of processing parameters were attempted, using a commercial laser sintering system (EOS P100, Germany), so that suitable parameters can be obtained for processing the parts. Combinations of laser powers of 13, 17, 18, 23 and 29 W and laser scan speed at 1500 and 2500 mm/s with a range of powder bed temperatures from 130 to 145 °C at five degree intervals and removal chamber temperature at 125, 130 and 135 °C were attempted in the initial trials. Laser count of 1 (single scan) and 2 (double scan) and scan spacing of 0.15 and 0.25 mm were attempted too. At a bed temperature of 142 °C and removal chamber temperature of 135 °C was found to be suitable in terms of powder spreading and multilayers sintering. However, powder removal and cleaning of the parts were diffecult. Therefore, low levels of laser powers of 6, 8, 10 and 12 W were attempted and were found to be suitable in terms of easiness of powder removal, cleaning, spreading of powder and reducing the effect of curling.

Rectangular parts (L = 80 mm × W = 10 mm × T = 4 mm) were built in x-y orientation with the long axis parallel to the x-axis, width parallel to the y-axis and thickness parallel to z-axis (i.e. build direction) as illustrated in Fig. 5. L, W and T were the length, width and thickness of LS parts respectively.

Laser powers of 6, 8, 10, 12 W were selected for processing in order to examine the effect of laser power on the flexural properties of the fabricated UHMWPE parts. All other parameters were kept constant as listed in Table 1. After building, all the parts were left in the machine for an hour and then were removed and left for cooling in the laboratory atmosphere for 24 h. Then the parts were air blown to remove the un-sintered powder.

Results from other work indicated that the microstructure, physical, mechanical properties and quality of the laser sintered parts are fundamentally affected by laser power, laser speed and scan spacing which are directly related to the amount of energy applied on the powder surface in the part bed. These parameters are seen as a function of energy density and for the purposes of this work, the incident energy density is taken to be [12]:

$$\text{Energydensity}(\text{J/mm}^2) = \text{Laserpower}/(\text{Scanspeed} \times \text{Scanspacing}) \quad (1)$$

4.2. Density

The bulk density (ρ_{Bulk}) of LS parts was determined using a volumetric method. The mass of the samples was determined by weighing the samples using a digital balance and the volume of the samples was determined using Vernier calliper measurement of dimensions as follows:

$$\rho_{\text{Bulk}} = \text{Mass}/\text{Volume} \quad (2)$$

The samples for density measurements were prepared by cutting the flexure test samples along the width with a razor blade in to approximately 10 mm length. Apparent density (ρ_{Apparent}) of sintered samples was determined using Helium Gas Pycnometer (Micromeritics AccuPyc II 1340, USA).

Density may also be expressed as relative density, which is defined as the ratio of the bulk density of the parts to the density of the material composing the parts (i.e. true density or theoretical density of the powder). A part which has 85% relative density will have 15% porosity. The relative density (ρ_{Relative}) was determined as follows:

$$\rho_{\text{Relative}} = (\rho_{\text{Bulk}}/\rho_{\text{True}}) \times 100 \quad (3)$$

In this study, the true density of the UHMWPE powder measured by helium gas pycnometer was 0.954 g/cm^3.

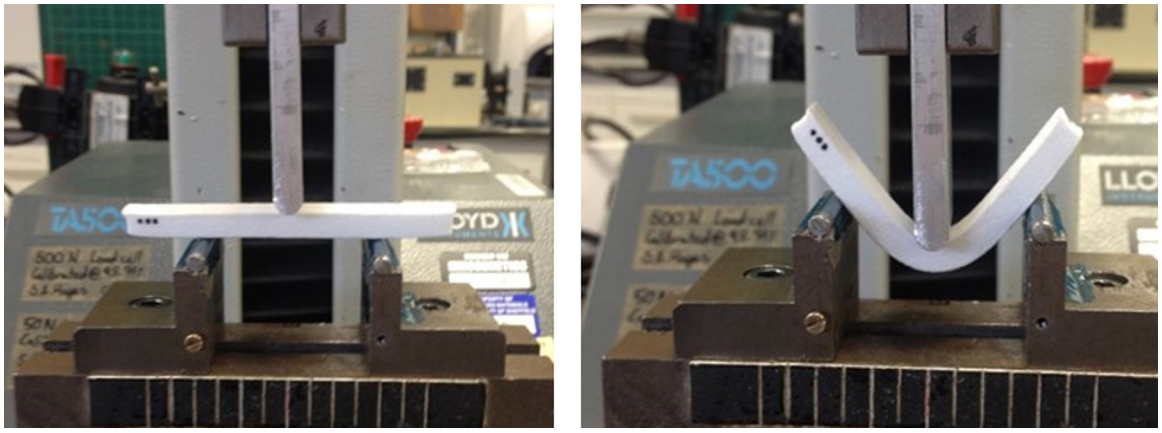

Fig. 6. Flexural test was performed on a Texture Analyser TA500.

4.3. Part dimensions

To investigate the effect of energy density on the dimensions of the LS parts, three different measurements (length, width and thickness) of the parts were taken. Three individual measurements of each dimension were taken and then an average value was generated for each part. Four LS parts were used for each set and then an average value for the sample length, width and thickness for each set was obtained. The dimensions were measured using Vernier calliper and compared to the dimensions of the input drawing. In this study, the linear and volumetric shrinkage of the laser-sintered parts were as follows:

$$\text{L-Shrinkage} = (L_o - L)/L_o \quad (4)$$

$$\text{W-Shrinkage} = (W_o - W)/W_o \quad (5)$$

$$\text{T-Shrinkage} = (T_o - T)/T_o \quad (6)$$

$$\text{V-Shrinkage} = (V_o - V)/V_o \quad (7)$$

where L_o (Length), W_o (Width) and T_o (Thickness) are the nominal size of the LS parts and L, W, and T are the actual size of length, width and thickness respectively. V_o ($L_o \times W_o \times T_o$) and V ($L \times W \times T$) are the nominal and actual volume of the sintered parts respectively.

4.4. Flexural properties

Flexural properties were examined by three-point bending tests (Fig. 6). The bending samples were designed with a nominal dimension of 80 mm long, 10 mm wide and 4 mm thick. The flexural strength was directly measured using the sintered parts without any post processing other than bead blasting. Three specimens for each set of parameters were tested and the average values were reported. Flexural tests were performed on a Texture Analyser TA500 (TM Lloyd Instruments, UK) fitted with a 500 N load cell. All tests were performed at ambient temperature with a constant cross-head speed of 2 mm/min and span length of 40 mm. After a significant deflection, the test samples take a V-shape, and load begins to drop. If the sample has not already failed and the load dropped to 40% then the test is stopped. In this study none of the sintered parts were ruptured during the three point bending tests but small cracks were observed on the bottom surface of some samples, at the centre-span, but they were not significant.

4.5. Scanning electron microscopy (SEM)

Microstructure of the LS samples was examined using a scanning electron microscope (Philips XL-20, Holland) at an accelerating voltage of 15 kV. Samples were cut out parallel to and 2–3 mm below the top surface, in the x-y plane, of the part and then were mounted on a sample's holder with an adhesive tape. All samples were gold sputtered before the examination.

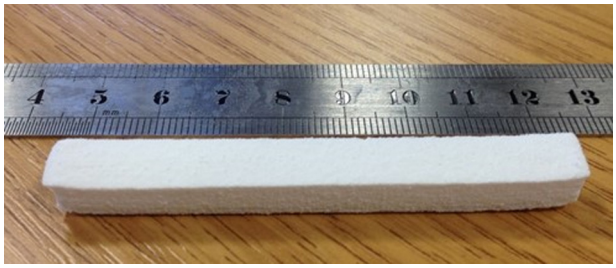

Fig. 7. Sintered part of UHMWPE fabricated using 10 W laser power.

Table 2
Densities of UHMWPE parts fabricated by LS.

Laser Power (watts)	Laser energy density (J/mm^2)	Bulk density (g/cm^3)	Apparent density (g/cm^3)	Relative density (%)
6	0.016	0.3353	0.9425	35.15
8	0.021	0.3682	0.9436	38.59
10	0.027	0.3748	0.9440	39.28
12	0.032	0.3550	0.9431	37.21

5. Parts manufacture and testing results and discussion

5.1. Laser sintering

UHMWPE multilayer parts were successfully manufactured using various laser power (LP). Sintered parts were manufactured with significant sintering between particles and layers and also good mechanical properties (Fig. 7).

5.2. Density

In LS process, the powder particles are sintered together by heat supplied by a laser and therefore the part density highly depends on the density of the energy provided by the laser [13]. The influence of laser energy density on density of the sintered parts is shown in Table 2 and presented in Figs. 8 and 9. LS parts have achieved bulk density in range of around 0.34–0.38 g/cm^3 which is higher than the bulk density of 0.20–0.25 g/cm^3 reported by the manufacturer (Celanese GUR® 2122 UHMWPE datasheet). The relative density of 35.15% was achieved with a laser energy density of 0.016 J/mm^2 (LP = 6 W) and the peak relative density value of

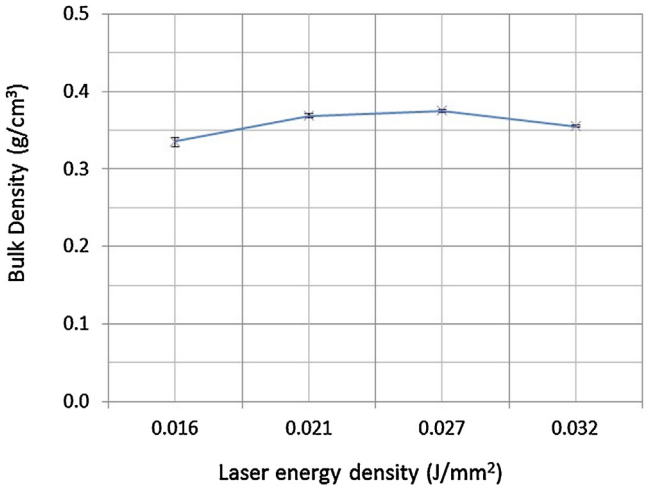

Fig. 8. Average effect of laser energy density upon the bulk density of the UHMWPE parts.

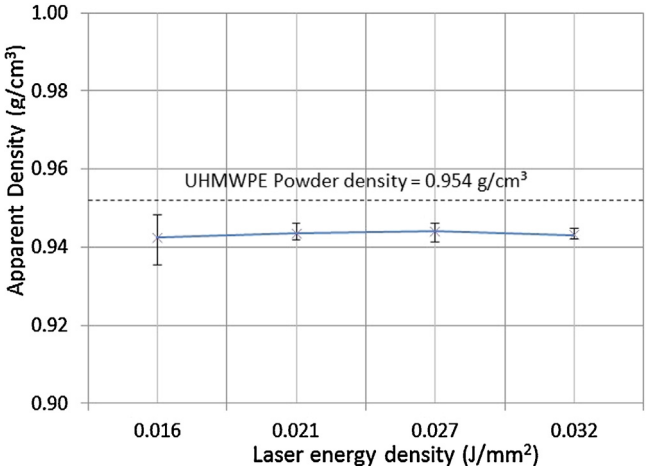

Fig. 9. Average effect of laser energy density upon the apparent density of the UHMWPE parts.

39.28% was achieved when laser energy density was maintained at about 0.027 J/mm^2 (LP = 10 W). However, the relative density seems to be slightly decreased to 37.21% when the laser energy density increased to 0.032 J/mm^2 (LP = 12 W). On a high energy density, thermal volatilization of polymer can be more severe and the mass of parts decreased [14], which decreases the density of the parts indicating an increasing of porosity. Further increase in energy density would cause more reduction in density due to probably polymer degradation and expansion of the voids by trapped gases. In general, low relative density of the UHMWPE fabricated parts has been observed for all sintered parts which indicates a high amount of pores developed by the laser sintering process.

5.3. Part dimensions

Results of the part dimensions measurements are shown in Table 3 and presented in Fig. 10. The investigation shows that the shrinking in the length and width was fluctuating with the increase of the energy density of the laser. However, the volume of the sintered UHMWPE parts was increasing with the increase of laser energy density which was due to high growth in the thickness of the parts (z-axis). Shrinkage in the length and width was evident and only one single experiment result where a growth in the width was observed at the highest energy density (i.e., 1.4% growth at

Table 3
Shrinkage of UHMWPE parts fabricated by LS with different energy densities.

Laser Power (watts)	Laser energy density (J/mm^2)	L-Shrinkage (%)	W-Shrinkage (%)	T-Shrinkage (%)	V-Shrinkage (%)
6	0.016	7.9	9.8	−60.06	−32.95
8	0.021	9.1	6.0	−64.31	−40.33
10	0.027	8.1	7.4	−67.77	−42.75
12	0.032	7.5	−1.4	−72.17	−61.45

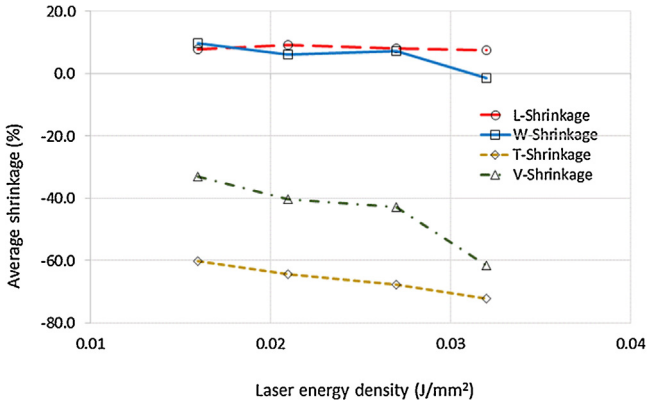

Fig. 10. Average shrinkage of UHMWPE parts fabricated by LS with different laser energy densities.

0.032 J/mm^2). The high growth was evident in the thickness with maximum value of 72.17% at the highest energy density. The volume growth reached a maximum value, 61.45%, when the laser energy density was 0.032 J/mm^2 (LP = 12 W). The maximum linear shrinkage was 9.1% and 9.8% in length and width, respectively.

Dimensional inaccuracy is a common occurrence when laser sintering polymer materials and it is still a major challenge [15]. These typical dimensional variations are due to inhomogeneous shrinkage during the building and cooling processes which leads to distortion in the sintered parts caused by stresses [16].

Many factors may contribute to shrinkage but mainly including materials, process parameters, and the geometries of parts produced [17]. On the other hand, growth in laser-sintered parts may also occur due to thermal inconsistencies within the powder bed. Goodridge et al. [5] highlighted the importance of pre-heating of the powder to avoid the curling phenomenon and also to achieve uniformity across the powder bed when sintering UHMWPE. In their study a Vanguard Laser Sintering machine from 3D System was used. This machine has two powder feed chambers fitted with a temperature controlled heater so that the powder can be heated before being spread across the build area. In our study we used EOS P100 machine in which there is no facility to pre-heat the powder before the deposition over the build bed. Therefore, high thermal gradients was expected when sintering UHMWPE and hence the high shrinkage.

This shrinkage depends on the temperature, at which the part is subjected to laser sintering. It is also affected by the length of time the powder bed retains heat (i.e., cooling), as well as the thickness of the powder layer [16].

It is widely acknowledged that part orientation is a significant factor that influences the dimensional accuracy of the part to be produced [17]. Part orientation has an effect on the material properties such as strength and shrinkage [18]. Goodridge et al. [5] has successfully produced UHMWPE sintered parts reporting dimensional accuracy of ±0.1 mm and the parts being built in vertical orientation (i.e. length being in the z-axis direction). In our study the parts were placed in x-y plane and the thickness being in z-axis (Fig. 5). Hopkinson and Sercombe [19] investigated the accuracy

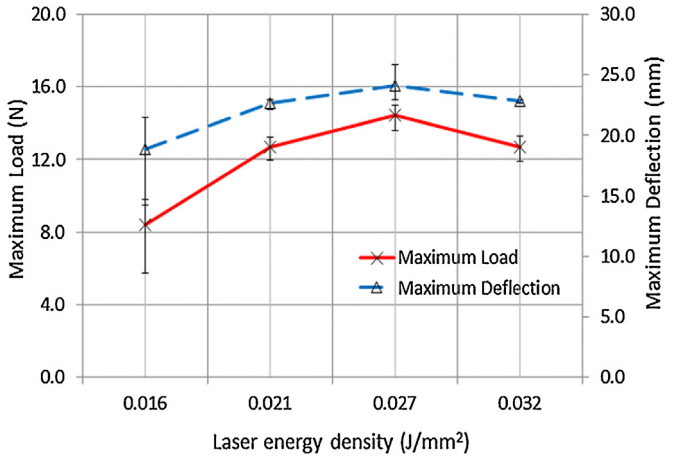

Fig. 11. Effect of laser energy density on maximum flexural load and deflection of UHMWPE parts.

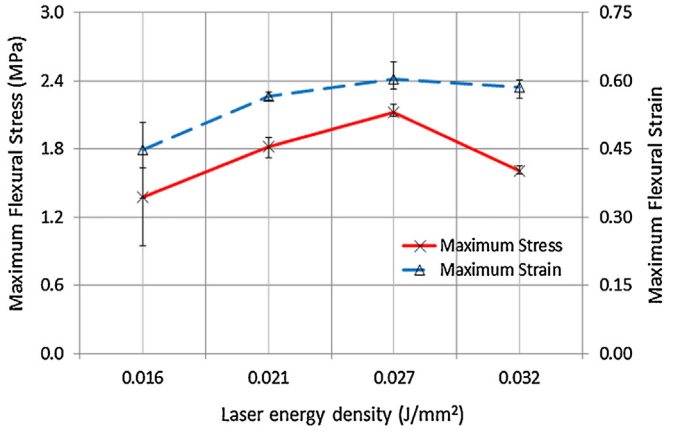

Fig. 12. Effect of laser energy density on maximum flexural stress and strain of UHMWPE parts.

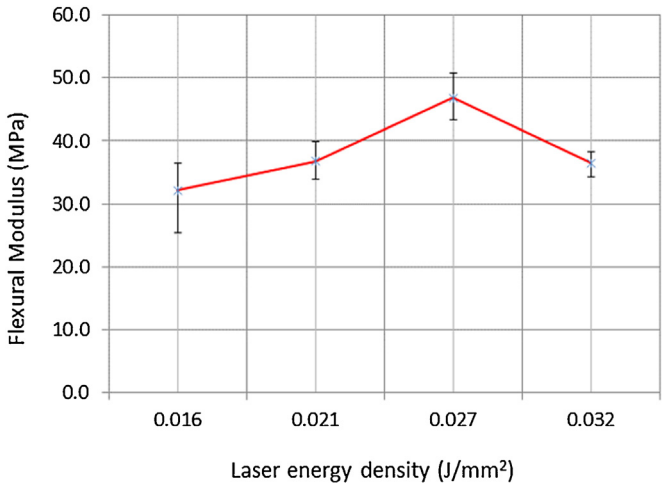

Fig. 13. Effect of laser energy density on maximum flexural modulus of UHMWPE parts.

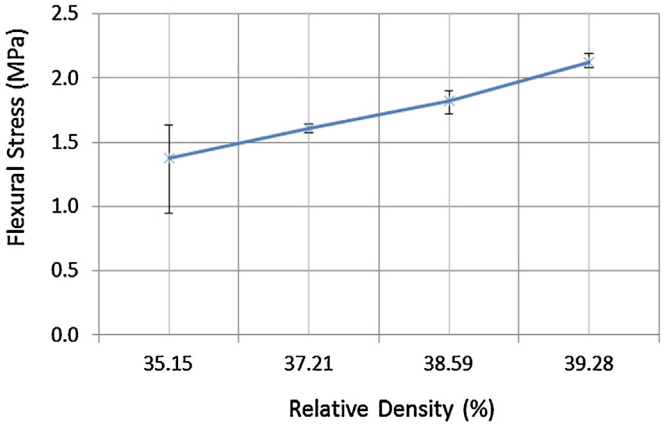

Fig. 14. Relative density v Flexural stress for UHMWPE sintered parts.

and the effect of part position on the shrinkage during indirect laser sintering of aluminium powder. They found that error in z-axis direction is more clearly apparent than in-plane errors. This phenomenon is called "Z-growth" which occurs as a result of the heat from the laser penetrates beyond the down facing surface to bond undesirable particles.

5.4. Flexural properties

Flexural strength was measured to examine the importance of LS energy density (i.e. laser power). The average effect of laser energy densities upon the flexural properties is shown in Table 4 and presented in Figs. 11 and 12.

The change trend of flexural strength is similar to the bulk density in Fig. 8. Higher laser energy density (ED) increases the flexural strength of the UHMWPE parts. With increasing bulk density the flexural strength increases. The maximum value of the flexural strength is 2.12 ± 0.05 MPa at an ED of 0.027 J/mm^2 (LP = 10 W). Results show that flexural strength is influenced by laser energy density and good flexural strength is still achieved with an ED of 0.016 J/mm^2 (LP = 6 W). A slightly lower strength is observed at ED of 0.032 J/mm^2 (LP = 12 W), due to a decrease in bulk density (Fig. 8). Fig. 13 clearly shows that the flexural modulus increased systematically with the increase of energy density. The peak flexural modulus value of 46.86 ± 3.07 MPa was achieved when laser energy density was maintained at about 0.027 J/mm^2 (LP = 10 W) and then began to drop at ED of 0.032 J/mm^2 (LP = 12 W). This drop is probably due to thermal degradation caused by an excessive exposure of the laser to the powder causing the particles to burn [20].

The results here show notable differences with the work carried out by Goodridge et al. [5] which studied the flexural properties of UHMWPE. The primary reason for this distinction is the significant difference in the manufacturing process between the present work and Goodridge et al. work. In their work the sintered parts were manufactured using Vanguard laser sintering machine equipped with temperature controlled heaters around the powder feed chambers. Pre-heating process of the powder is crucial in laser sintering and has significant effect in reducing the thermal gradients. Furthermore, Goodridge et al. used a vertical orientation when building the parts and this probably would minimise the dimension inaccuracy and shrinkage but may lead to a negative effect on strength.

Flexural strength and modulus vary directly with density and low density reduces maximum strengths due to high porosity. The flexural test results show that the flexural stress and modulus increase with increase in relative density as shown in Figs. 14 and 15.

5.5. Scanning electron microscopy (SEM)

Fig. 16 shows representative SEM micrographs of the surface of the porous sintered samples from the UHMWPE powder at laser power of 10 W. The porous structure is seen to form between

the powder agglomerations, forming irregular pores connected together and a heterogeneous distribution.

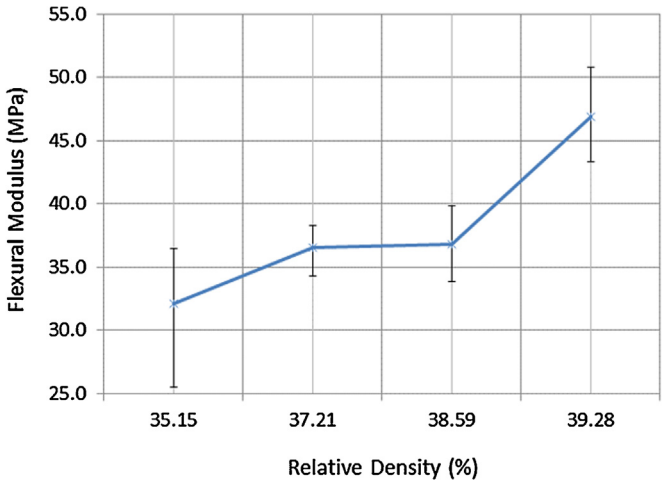

Fig. 15. Relative density v Flexural modulus for UHMWPE sintered parts.

6. Conclusions

Although processing UHMWPE using laser sintering was challenging (due to a narrow super-cooling process window), good parts were fabricated successfully at various laser power using a commercial machine EOS P100 with laser energy density range between 0.016 and 0.032 J/mm^2. The average flexural strength of the sintered parts increased with increase in laser energy density up to 0.027 J/mm^2 with a maximum value of the flexural strength of 2.12 ± 0.05 MPa. The highest Young's modulus value achieved was 46.86 ± 3.07 MPa when the laser energy density was maintained at about 0.027 J/mm^2. The sintered parts achieved bulk density in range of around 0.34–0.38 g/cm^3 which is higher than the bulk density of 0.20–0.25 g/cm^3 reported by the manufacturer (Celanese GUR® 2122 UHMWPE datasheet). Based on the findings of this study, shrinking in the length and width was evident. The volume of the sintered UHMWPE parts increased with the increase of laser energy density due to the growth in the thickness of the parts. The dimensional inaccuracy is still a major challenge when laser sintering polymer materials.

Acknowledgements

The authors would like to thank Mr. Peter Burke from Ticona GmbH (Celanese, Germany) for the generous supply with the UHMWPE powder for this study. The authors also would like

Table 4
Flexural properties of UHMWPE parts fabricated by LS.

Laser Power (watts)	6	8	10	12
Laser energy density (J/mm^2)	0.016	0.021	0.027	0.032
Maximum Load (N)	8.43 ± 1.89	12.67 ± 0.52	14.46 ± 0.60	12.71 ± 0.59
Maximum Deflection (mm)	18.83 ± 3.29	22.64 ± 0.36	24.12 ± 1.28	22.87 ± 0.14
Maximum Flexural Stress (MPa)	1.37 ± 0.30	1.82 ± 0.07	2.12 ± 0.05	1.61 ± 0.03
Maximum Flexural Strain	0.45 ± 0.08	0.57 ± 0.01	0.60 ± 0.03	0.59 ± 0.02
Flexural Modulus (MPa)	32.12 ± 4.78	36.82 ± 3.00	46.86 ± 3.07	36.53 ± 1.67

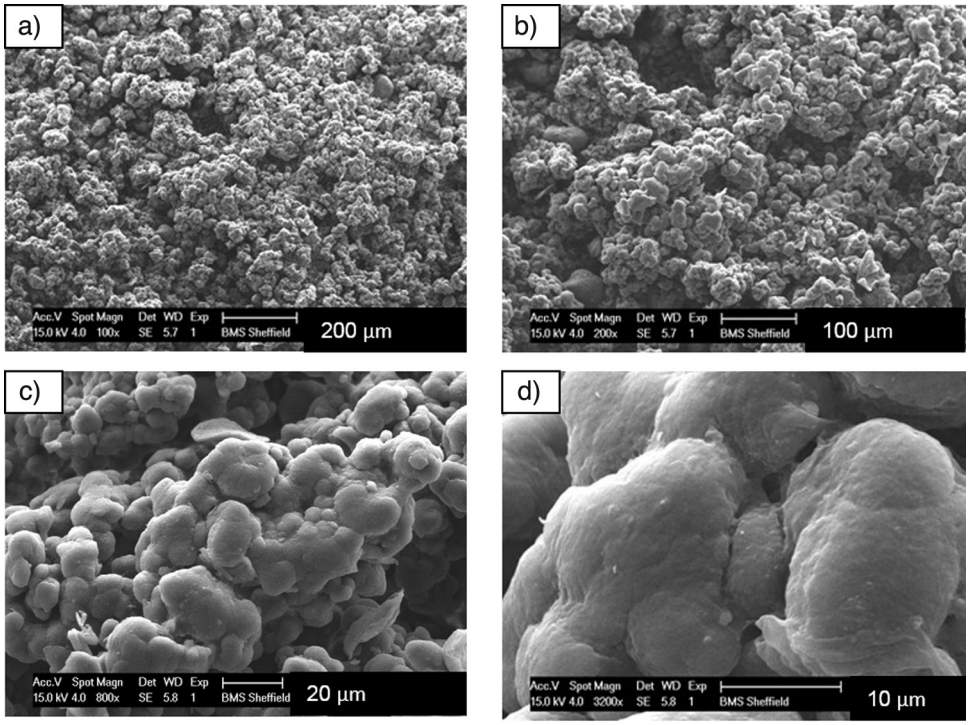

Fig. 16. SEM micrographs of the sintered part of UHMWPE at laser power of 6 W magnifications: (a) 100×, (b) 200×, (c) 800× and (d) 3200×.

to acknowledge the research funding from the Engineering and Physical Sciences Research Council (EPSRC) of Great Britain (grant number EP/M507611/1). Further contribution from the industrial sponsor (Unilever plc, UK) is also acknowledged with appreciation.

References

[1] G.H. Michler, V. Seydewitz, M. Buschnakowski, L.P. Myasnikowa, E.M. Ivan'kova, V.A. Marikhin, Y.M. Boiko, S. Goerlitz, Correlation among powder morphology: compactability, and mechanical properties of consolidated nascent UHMWPE, J. Appl. Polym. Sci. 118 (2) (2010) 866–875.
[2] X. Liang, X. Wu, K. Zeng, B. Xu, S. Wu, H. Zhao, B. Li, S. Ruan, Micro ultrasonic powder molding for semi-crystalline polymers, J. Micromech. Microeng. 24 (4) (2014) 045014.
[3] D.L. Bourell, T.J. Watt, D.K. Leigh, B. Fulcher, Performance limitations in polymer laser sintering, Phys. Procedia 56 (2014) 147–156.
[4] ISO/ASTM Standard 52900, Additive Manufacturing – General Principles – Terminology, ISO/ASTM International, Switzerland, 2015.
[5] R.D. Goodridge, R.J.M. Hague, C.J. Tuck, An empirical study into laser sintering of ultra-high molecular weight polyethylene (UHMWPE), J. Mater. Process. Technol. 210 (1) (2010) 72–80.
[6] N. Hopkinson, R. Hague, P. Dickens, Rapid Manufacturing: An Industrial Revolution for the Digital Age, Wiley, 2006.
[7] S.M. Kurtz, UHMWPE Biomaterials Handbook: Ultra High Molecular Weight Polyethylene in Total Joint Replacement and Medical Devices, Academic Press, 2009.
[8] A.d.A. Lucas, J.D. Ambrósio, H. Otaguro, L.C. Costa, J.A.M. Agnelli, Abrasive wear of HDPE/UHMWPE blends, Wear 270 (9-10) (2011) 576–583.
[9] A. Kelly, Concise Encyclopedia of Composite Materials, Elsevier Science, 2012.
[10] Q. Zhang, M. Jia, P. Xue, Study on molding process of UHMWPE microporous filter materials, J. Appl. Polym. Sci. 126 (4) (2012) 1406–1415.
[11] J.T. Rimell, P.M. Marquis, Selective laser sintering of ultra high molecular weight polyethylene for clinical applications, J. Biomed. Mater. Res. 53 (4) (2000) 414–420.
[12] J.D. Williams, C.R. Deckard, Advances in modeling the effects of selected parameters on the SLS processnull, Rapid Prototyp. J. 4 (2) (1998) 90–100.
[13] S. Dupin, O. Lame, C. Barrès, J.-Y. Charmeau, Microstructural origin of physical and mechanical properties of polyamide 12 processed by laser sintering, Eur. Polym. J. 48 (9) (2012) 1611–1621.
[14] K. Liu, Y. Shi, W. He, C. Li, Q. Wei, J. Liu, Densification of alumina components via indirect selective laser sintering combined with isostatic pressing, Int. J. Adv. Manuf. Technol. 67 (9–12) (2013) 2511–2519.
[15] S.P. Soe, D.R. Eyers, R. Setchi, Assessment of non-uniform shrinkage in the laser sintering of polymer materials, Int. J. Adv. Manuf. Technol. 68 (1–4) (2013) 111–125.
[16] K. Manetsberger, J. Shen, J. Muellers, Compensation of non-linear shrinkage of polymer materials in selective laser sintering, in: Solid Freeform Fabrication Symposium, Auston, Texas, USA, 2001.
[17] K. Senthilkumaran, P.M. Pandey, P.V.M. Rao, Influence of building strategies on the accuracy of parts in selective laser sintering, Mater. Des. 30 (8) (2009) 2946–2954.
[18] S. Danjou, P. Köhler, Determination of optimal build direction for different rapid prototyping applications, in: Proceedings of the 14th European Forum on Rapid Prototyping, Ecole Centrale Paris, 2009.
[19] N. Hopkinson, T.B. Sercombe, Process repeatability and sources of error in indirect SLS of aluminium, Rapid Prototyp. J. 14 (2) (2008) 108–113.
[20] B. Caulfield, P.E. McHugh, S. Lohfeld, Dependence of mechanical properties of polyamide components on build parameters in the SLS process, J. Mater. Process. Technol. 182 (1–3) (2007) 477–488.